Large Phase-by-Phase Modulations in Atomic Interfaces

M. Artoni[1,2,3] and A. Zavatta[2]
[1]European Laboratory for Nonlinear Spectroscopy (LENS), I-50019 Sesto Fiorentino, Firenze, Italy
[2]Istituto Nazionale di Ottica (INO-CNR), I-50125 Firenze, Italy
[3]Department of Engineering and Information Technology, Brescia University, I-25133 Brescia, Italy
(Received 16 March 2015; published 10 September 2015)

Phase-resonant closed-loop optical transitions can be engineered to achieve broadly tunable light phase shifts. Such a novel phase-by-phase control mechanism does not require a cavity and is illustrated here for an atomic interface where a classical light pulse undergoes radian level phase modulations all-optically controllable over a few micron scale. It works even at low intensities and hence may be relevant to new applications of all-optical weak-light signal processing.

DOI: 10.1103/PhysRevLett.115.113005 PACS numbers: 32.80.Qk, 42.50.Gy

All refractive optics of *macroscopic* media, including basic tools such as lenses, work by applying spatially varying phase shifts of several radians to incoming light beams. The ability, on the other hand, to control phases and relative phases over the short length scales of *microscopic* media is a challenging task in optics and of obvious relevance to modern microscopy [1], information processing [2–4], and micro- and nanoscale optics [5,6]. In quantum systems, e.g., large and controllable optical phase shifts have long remained elusive and only recently appreciable shifts have been observed from atoms [7], molecules [8], trapped ions [9], and superconducting qubits [10]. It's even less obvious how to attain large and controllable optical shifts working at low-light levels or with the tiny optical powers of several or a few *photons*. This requires unpractical propagation distances, often overcome by using multipass high-finesse optical cavities [11], or strong enhancements of the weak photon-photon nonlinear interactions. Electromagnetically induced transparency, e.g., is commonly used in trapped atomic samples to enhance the weak Kerr effect responsible for the photon-photon interaction, namely, through a significant reduction of the photon's propagation speed. Within this context, multilevel atom configurations driven to attain large cross-phase-modulation effects have been extensively studied [12–16] and over the years various demonstrations [17–20] of phase shifts, which may even reach the size of a radian [21–23], have been carried out yet at the price of fairly large light intensities. Conversely, this seems to confirm early predictions that large shifts through enhancement of Kerr nonlinearities at low-light levels or even down to the single-photon level [24,25] are unlikely.

Here we discuss a physical mechanism to achieve radian-level shifts in the phase of an optical field across the tiny length scales of an atomic interface [26]. We show that the phase of a weak narrow band *signal* wave packet can be steered by easily changing the interface driving parameters or by means of another weak narrow band copropagating *control* wave packet. The signal phase may be preserved or set to acquire continuously variable shifts reaching π radians. This can be done all-optically over a few microns.

The proposal is illustrated for classical coherent states and builds on ideas of resonant effects occurring in atomic transitions with a closed excitation loop, where the resonant conditions hinge not only on frequencies but also on the phase of the exciting lasers [27–29]. The phase control parameters and interface characteristics are described in Figs. 1(a) and 1(b). The control mechanism does not require a cavity and is in principle efficient even for weak classical fields. Such an approach may be relevant to new applications of all-optical low-light signal processing for communications and information [39] including all-optical switching [40] as exemplified, e.g., in Fig. 1(c).

The shift in the phase of the signal (ω_m) across the interface in the presence of the control wave packet (ω_p) is computed here within the general framework of quantum electromagnetic theory [41] through the phase of the signal electric field expectation value $\langle \hat{E}_m^+(z,t)\rangle$ [33]. The operator $\hat{E}_m^+(z,t)$ is obtained as a one-dimensional continuous-mode Heisenberg field operator solution of a system of coupled equations describing the signal and control joint dynamics through the interface. Such a field can be expressed as a superposition of signal and control free-space field operators weighted by the atomic-medium electric fields *amplitudes* $\mathcal{E}_{mm}$ and $\mathcal{E}_{mp}$ [33,42]. Each amplitude's expression is involved, yet for wave packets [Fig. 1(b)] double-resonant with (i) a nearly resonant transition and with (ii) a Raman transition for which $\{\delta_p,\gamma_2\} \ll \Delta \ll |\Omega_c|^2/\gamma_3$, we can rewrite $\mathcal{E}_{mm}$ and $\mathcal{E}_{mp}$ as suitable superpositions [33,42] of two plane–waves whose frequency-dependent wave vectors are determined by the refractive index n_- and n_+ exhibited, respectively, on the nearly-resonant transition and on the far-detuned Raman transition. Upon averaging $\hat{E}_m^+(z,t)$ over a continuous-mode coherent state $|\{\alpha_m,\alpha_p\}\rangle$ [43], representing our incident wave packets each with a Gaussian frequency

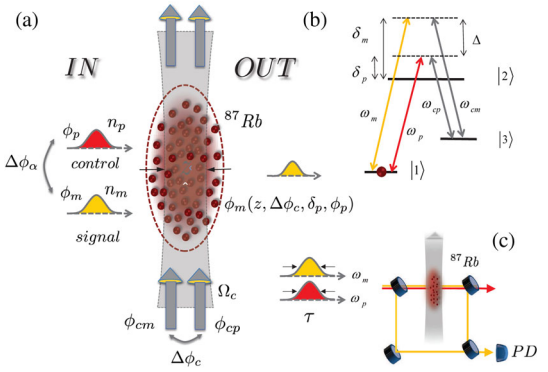

FIG. 1 (color online). (a) Phase Control. Two *weak* coherent wave packets ω_m and ω_p, with equal initial intensities ($n_m = n_p$) and length ($\mathcal{L}$), and two coupling beams ω_{cm} and ω_{cp} couple to an atomic interface of length z [30]. The couplings relative phase $\Delta\phi_c$, the phase ϕ_p and detuning δ_p of the control wave packet are used to steer the phase ϕ_m of the signal wave packet. Here ϕ_m (ϕ_p) and n_m (n_p) are the initial mean phase angle and mean photon number of the coherent state excitation α_m (α_p) in the mode m (p). The two couplings Rabi frequency are fixed at $\Omega_c = 2\gamma_2$ and the Raman detuning at $\Delta = 20\gamma_2$. (b) The interface. The level scheme corresponds to the transition $5\,^2S_{1/2} \rightarrow 5\,^2P_{3/2}$ (^{87}Rb D_2 line) at $\lambda_{21} = 780.24$ nm with decay rates $\gamma_2 = 2\pi \times 6$ MHz and $\gamma_3 = 2\pi \times 1$ kHz. The wave packets with a bandwidth $c/\mathcal{L} \sim 1/\tau \lesssim \gamma_2 \ll \Delta$ are double resonant with the couplings ($\omega_m - \omega_{cm} \simeq \omega_p - \omega_{cp}$) through a nearly resonant ($\delta_p \simeq \delta_{cp} \lesssim \gamma_2$) transition and a far off-resonant ($\delta_m \simeq \delta_{cm} = \Delta$) Raman transition between the two hyperfine grounds $|1\rangle$ and $|3\rangle$. (c) Measurement. Mach-Zehnder setup used to measure $\phi_m(z,t)$ at the photodetector (PD). The interferometer may also be used to implement a low-light optical switch [33].

distribution $\xi_{m,p}(\omega) = (\mathcal{L}^2/2\pi c^2)^{1/4} e^{-\mathcal{L}^2(\omega-\omega_{m,p})^2/4c^2}$, and working out the phase of $\langle \hat{E}_m^+(z,t)\rangle$ we obtain the shift accumulated at time t across an interface of length z [33],

$$\phi_m(z,t) = 2\Phi + \arg[Z(z,t)] \simeq \Phi - |\zeta| - \tan^{-1}\left[\frac{\cos[\delta(z) + 2|\zeta|]}{\sin[\delta(z) + 2|\zeta|] + \frac{\mathcal{E}^-(z,t)\cos\Phi}{\mathcal{E}^+(z,t)\sin\Phi}}\right]. \quad (1)$$

We denote by $2\Phi = (\Delta\phi_c - \Delta\phi_\alpha)$ the difference between the couplings relative phase $\Delta\phi_c = \phi_{cm} - \phi_{cp}$ and the two wave packets initial relative phase $\Delta\phi_\alpha = \phi_m - \phi_p$ [Fig. 1(a)]. The complex function [44]

$$Z(z,t) = n_p^{1/2} I_{mp}(z,t) + e^{-i\{2\Phi + \Delta[(z/c)-t]\}} n_m^{1/2} I_{mm}(z,t) \quad (2)$$

comprises the frequency convolution I_{mp} (I_{mm}) between the electric field amplitudes $\mathcal{E}_{mp}$ ($\mathcal{E}_{mm}$) and the mode frequency distributions ξ_p (ξ_m) that arise from computing $\langle \hat{E}_m^+(z,t)\rangle$. For the specific driving conditions (i and ii) we adopt here one has [33]

$$I_{mp}(z,t) \simeq [e^{i\eta_-(\omega_p z/c)}\mathcal{E}^-(z,t) - \{- \rightarrow +\}]e^{-i\omega_p t}, \quad (3)$$

where the two envelopes

$$\mathcal{E}^\pm(z,t) = e^{-\kappa_\pm(\omega_p z/c)} e^{-c^2[t-(z/v_\pm)]^2/\mathcal{L}^2}, \quad (4)$$

propagate at different group velocities ($v_\pm$) and damp over different lengths ($\propto \lambda_p \kappa_\pm^{-1}$), with $\eta_\pm$ ($\kappa_\pm$) being the real (imaginary) part of the refractive index $n_\pm$. With the help of I_{mp} and I_{mm} [45] one obtains from Eq. (2) the signal shift $\phi_m(z,t)$, which can be described to a very good approximation by the last expression in Eq. (1), with $\zeta = i\gamma_3\Delta/|\Omega_c|^2$. Such a simplified expression indicates that variations mainly occur through the mismatch $\delta(z) = (\eta_+ - \eta_-)\omega_p z/c$, giving rise to space oscillations with period $L_{\rm osc} \simeq \Delta/\gamma_2(N/V)\lambda_o^2$, and through the second term in the denominator of the inverse-tangent function in Eq. (1), giving rise instead to space-time modulations. The former are determined by the phase velocities $c/\eta_\pm$ while the latter are determined by the envelopes $\mathcal{E}^\pm(z,t)$ and Φ. In particular, at any time t and z the shift $\phi_m(z,t)$ will be affected by the external *phase* difference Φ and by the interface optical response, through the control *detuning* δ_p. Both parameters can be changed independently, providing a wide range of control over the signal phase as we discuss below.

Phase modulations.—Consider first some *specific* values of Φ, i.e.,

$$\Phi = 0 \quad \text{or} \quad \Phi = \frac{\pi}{2}. \quad (5)$$

The last term in Eq. (1) practically vanishes in the first case, a situation that is relevant when the phase $\phi_m(z,t)$ needs to be preserved through the interface ($|\zeta| \ll 1$). The fact that space-time propagation effects have in this case little impact on the signal shift physically arises from dark-state *matching*. This can be understood by supposing that each of the two optical fields creates its own dark state through the corresponding coupling beam. When $\Phi = 0$ the two dark states exactly *match* to one another [46], the atoms loosely couple to the signal and control field in a regime of reduced absorption and slow light propagation. As a result the interface has a negligible steady effect on the shift. Conversely, when $\Phi = \pi/2$ the last term in Eq. (1) does not vanish and $\phi_m(z,t)$ increase (nearly) linearly with z, exhibiting a π-radian change over half a period $L_{\rm osc}$. This is important instead when exactly a π-phase change is sought after. In this case, however, the dark state *mismatch* is such that the atoms strongly couple to the fields and the signal quickly dissipates through the sample, making the shift observable only over a $10 - 20$ μm long interface [33].

The case of *arbitrary* Φ's, no longer subject to the restrictions [Eq. (5)], is less intuitive. One expects continuous *space-time* variations of $\phi_m(z,t)$ which we examine here at a given time t_0 of the signal wave packet propagation and for a typical range of atomic interface

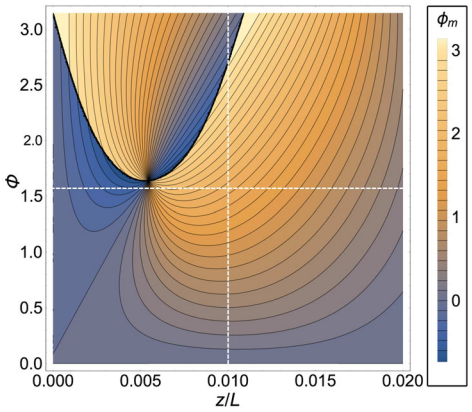

FIG. 2 (color online). Signal phase modulations accumulated at time $t_0 = 0.1\tau$ by a narrow band signal Gaussian wave packet of duration $\tau = 5.2\ \mu$s for arbitrary interfaces of lengths z and phases Φ. Each curve represents values $\{z, \Phi\}$ for which $\phi_m(z, t_0)$ has the same value. Phases are in rad with an atomic density $N/V \simeq 10^{13}$ cm^{-3} and a length scale $L = 1$ mm. All other parameters are as in Fig. 1.

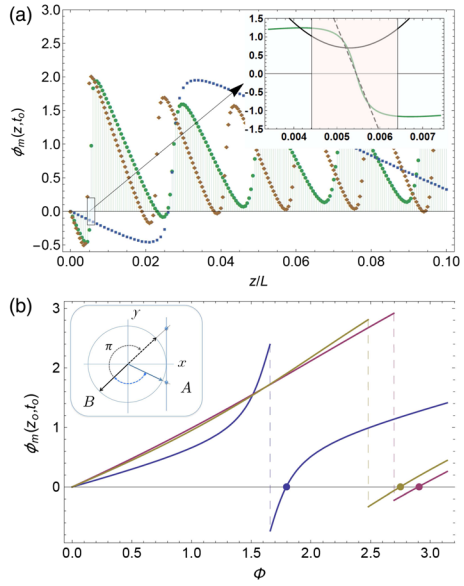

FIG. 3 (color online). (a) Signal phase $\phi_m(z, t_0)$ vs z ($\Phi = \pi/4$) when $\delta_p = 0$ and $N/V \simeq 10^{13}$ cm^{-3} (green), $\delta_p = 0$ and $N/V \simeq 5 \times 10^{12}$ cm^{-3} (blue), $\delta_p = 0.03\gamma_2$ and $N/V \simeq 10^{13}$ cm^{-3} (brown). Inset: Inverse tangent term (green) in Eq. (1) around $z \simeq 0.0054L$ (box). Large shifts arise from a swift change in sign of the numerator (dash) over μm length scale where the denominator (solid) has only smooth variations. (b) Signal phase $\phi_m(z_0, t_0)$ vs Φ when $z_0 = 0.006L$ (blue), $z_0 = 0.01L$ (violet), and $z_0 = 0.14L$ (green). For $z_0 = 0.01L$ the phase undergoes a π shift for $\Phi \simeq 2.9$ (blue-dot). Inset: The phase plotted π jumps are due to a quadrant swap [33].

lengths z and arbitrary phases Φ. The results, reported in Fig. 2 for a setup of ultracold ^{87}Rb [47], show broad tunability with Φ, meaning that signal phase manipulation can be achieved directly [48] by changing *either* the couplings phases ($\Delta\phi_c$) *or* the control pulse phase (ϕ_p). One of these characteristic phase patterns is illustrated for a fixed value of Φ in Fig. 3(a). Each point (green dots) corresponds to a length z and regions with a sparse point distribution correspond to the steepest phase gradients. We also examine in this case how the atom density (blue dots) [49] and the control pulse detunings δ_p (brown dots) affect the signal phase. Optically thicker (thinner) interfaces in general exhibit shorter (longer) modulations with a sharper (smoother) rise since $L_{\rm osc} \propto (N/V)^{-1}$. Rather small δ_p's, on the other hand, are sufficient to shrink the pattern of the phase swiftly moving the maxima at z's for which one would observe nearly no shift in the case of a vanishing δ_p. Notice that in all cases steep changes take place over ramps ranging from a few to several μm [Fig. 3(a), inset]. We, finally, show phase patterns for arbitrarily fixed lengths z in Fig. 3(b) where the signal phase undergoes *any* required shift between 0 and π as Φ is varied [48]. We report, in particular, the values of Φ (color dots) for which the phase undergoes a complete π-change.

Discussion.—Any viable all-optical physical mechanism to control steep phase changes on short length scales requires broad tunability, steep gradients, basic control optics, and low loss. The results above indicate that these requirements are essentially met. We focus now on emphasizing some key features

First, the mechanism by which two wave packets can steer one another's phase to large modulations hinges on *propagation*. The steep shifts in Fig. 3, e.g., physically arise from the joint propagation of the two wave packets' electric fields $E_m^+(z, t)$ and $E_p^+(z, t)$, hence their phases, specifically occurring when the propagation of the two fields makes the numerator of the inverse tangent argument in Eq. (1) undergo rapid sign changes in region(s) where the denominator is smooth [see Fig. 3(a), inset]. This phase-shift effect is then associated with the process of energy swapping [50] between the two frequency channels of the interface taking place in a regime of slow light propagation via the common spin coherence $|1\rangle$-$|3\rangle$ [33].

Second, for identical wave packets the shift $\phi_m(z, t)$ is *independent* of the intensity [51]. This leads to the noteworthy result that the mechanism may work in principle for very weak classical signal (control) field excitations. Thus, in proximity of a steep phase-change, radian-level shifts in the signal phase may in general be obtained at a much reduced interaction strength than it would be required to achieve through typical non-linear cross-phase-modulations [23]. Within our twofold closed-loop interface configuration, steep shifts in fact are largely determined by the combined dynamics of two wave packet envelopes rather than their intensities, as clearly embedded in Eq. (1).

Large shifts are not new. The Gouy shift, whereby light passing through a focus will undergo a π shift [52], or the π-phase advance that blue detuned light will experience when tuned through an atomic resonance [9] are well

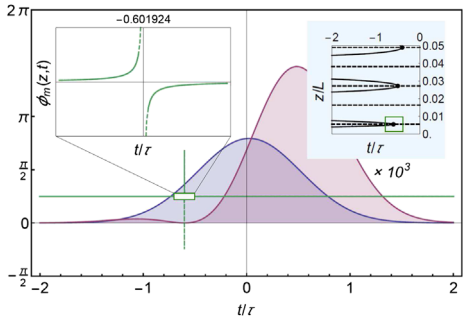

FIG. 4 (color online). Signal phase $\phi_m(z_0,t)$ (green line) vs time for an interface of length $z_0 = 5.4$ μm and intensity of the signal (purple fill) and control (blue fill) pulses. The signal drops to zero at $t_0 \simeq -0.6\tau$. Right, inset: Loci where the denominator (continuous) and numerator (dashed) of the inverse tangent term in Eq. (1) are zero. At the intersections (dots) the inverse tangent is undefined and the field intensity is zero. Left, inset: Enlargement of the box in the main frame showing the signal phase singularity corresponding to the lower intersection point inside the green square box shown in the right inset. The singularity appears around the point $t_0 = -0.6\tau \pm \delta t$ ($\delta t = 5 \times 10^{-11}\tau$).

known. At variance with these instances where distances as large as a few Rayleigh ranges [52] or complicated architectures with a string of atoms [7] or molecules [8] spread over a few hundred of nanometers are needed to achieve sizable shifts and yet with sizable intensities, our method works *even* for weak intensities [53]. This phase-resonant excitation free-space mechanism, in addition, does not require demanding confinements [6–9] to control both the strength and the spatial range over which changes in $\phi_m(z,t)$ occur but only basic optics entailing phases besides detunings [see Fig. 3(b)].

Third, the control mechanism affects not only phases but also the mode intensity; characteristic space-time dependent power densities are reported in Ref. [33]. We find it instructive to examine here the joint time-dependent evolution of both m and p mode intensities together with the phase accumulated by the signal. This is done in Fig. 4 where $\phi_m(z_0,t)$ is seen to remain almost constant along the pulse temporal profile, *except* close to a region around t_0 where a phase singularity [54] occurs (inset, left). Here the p mode (blue) is mostly populated while the other shows a residual profile around t_0 arising from not-a-perfect swapping. Both real and imaginary parts of the m-mode amplitude $Z(z,t)$, and hence its intensity [33], vanish at t_0, the phase remaining then undefined. In general, there are more of these singularities occurring precisely at the crossings points (black dots) of the contour lines in Fig. 4 (inset, right). The overall space-time evolution of the signal phase and its singularities are further illustrated through an animation in Ref. [33].

Outlook.—Managing phases of weak optical fields over short distances is a challenge in different research areas [1–10]. In multiatom ensembles, Kerr enhancement, e.g., is often used to achieve appreciable phase modulations, yet when working in the low-light level regime there exists an upper limit of the order of a fraction of a radian per photon [24]. Other interesting forms of enhancement in warm [55] or cold Rydberg atoms [56,57] can also be envisaged. By exploiting, instead, phase-sensitive coherent excitations in a multilevel-atom interface (see Fig. 1), shifts between 0 and π can be continuously controlled by direct optical engineering of the interface, e.g., by adjusting the coupling beams phases $\Delta\phi_c$ while fixing either of the two pulse control parameters $\{\delta_p, \phi_p\}$ or by reversibly fixing $\Delta\phi_c$ while adjusting either of $\{\delta_p, \phi_p\}$.

Phase control remains efficient here even for *weak* fields; the conditions [Eq. (5)], e.g., may be relevant to implementations of a conditional π-phase shift between two (very) weak classical pulses across the interface [58]. Finally, our results for Rb atoms adapt to cold-atom photonic crystal-fiber interfaces [59,60] or to solid interfaces [58,61–63], to miniaturized (micrometer-sized) atomic vapor cells [31,64] or to crystals doped with rare-earth-metal ions [58] or with nitrogen-vacancy color centers [65] where similar three-level two-fold interaction configurations exist.

This work was partially supported by European Union under the CHIST-ERA project QSCALE (Quantum Technologies for Extending the Range of Quantum Communications) and by the Italian Ministry of Education, University and Research under "X-Nano" project (Grant No. DM45975).

[1] *Biomedical Optical Phase Microscopy and Nanoscopy*, 1st ed. edited by N. Shaked, Z. Zalevsky, and L. Satterwhite (Academic Press, New York, 2012).
[2] L. Duan, M. Lukin, J. Cirac, and P. Zoller, Nature (London) **414**, 413 (2001).
[3] Q. A. Turchette, C. J. Hood, W. Lange, H. Mabuchi, and H. J. Kimble, Phys. Rev. Lett. **75**, 4710 (1995).
[4] M. Nielsen and I. Chuang, *Quantum Computation and Quantum Information* (Cambridge University Press, Cambridge, England, 2004).
[5] Q. Xu, P. Dong, and M. Lipson, Nat. Phys., **3**, 406 (2007).
[6] I. Fushman, D. Englund, A. Faraon, N. Stoltz, P. Petroff, and J. Vučković, Science **320**, 769 (2008).
[7] S. A. Aljunid, M. K. Tey, B. Chng, T. Liew, G. Maslennikov, V. Scarani, and C. Kurtsiefer, Phys. Rev. Lett. **103**, 153601 (2009).
[8] M. Pototschnig, Y. Chassagneux, J. Hwang, G. Zumofen, A. Renn, and V. Sandoghdar, Phys. Rev. Lett. **107**, 063001 (2011).
[9] A. Jechow, B. G. Norton, S. Händel, V. Blūms, E. W. Streed, and D. Kielpinski, Phys. Rev. Lett. **110**, 113605 (2013).
[10] O. Astafiev, A. M. Zagoskin, A. A. Abdumalikov, Y. A. Pashkin, T. Yamamoto, K. Inomata, Y. Nakamura, and J. S. Tsai, Science **327**, 840 (2010).
[11] J. Kerckhoff, M. A. Armen, D. S. Pavlichin, and H. Mabuchi, Opt. Express **19**, 6478 (2011).
[12] H. Schmidt and A. Imamogdlu, Opt. Lett. **21**, 1936 (1996).

[13] M. D. Lukin and A. Imamoğlu, Phys. Rev. Lett. **84**, 1419 (2000).
[14] A. Raczynski and J. Zaremba, Opt. Commun. **209**, 149 (2002).
[15] S. Li, X. Yang, X. Cao, C. Zhang, C. Xie, and H. Wang, Phys. Rev. Lett. **101**, 073602 (2008).
[16] A. Raczyński, J. Zaremba, S. Zielińska-Kaniasty, M. Artoni, and G. C. La Rocca, J. Mod. Opt. **56**, 2348 (2009).
[17] H. Kang and Y. Zhu, Phys. Rev. Lett. **91**, 093601 (2003).
[18] H.-Y. Lo, P.-C. Su, and Y.-F. Chen, Phys. Rev. A **81**, 053829 (2010).
[19] B.-W. Shiau, M.-C. Wu, C.-C. Lin, and Y.-C. Chen, Phys. Rev. Lett. **106**, 193006 (2011).
[20] M. Hosseini, S. Rebic, B. M. Sparkes, J. Twamley, B. C. Buchler, and P. K. Lam, Light Sci. Appl. **1**, e40 (2012).
[21] Y.-F. Chen, C.-Y. Wang, S.-H. Wang, and I. A. Yu, Phys. Rev. Lett. **96**, 043603 (2006).
[22] H.-Y. Lo, Y.-C. Chen, P.-C. Su, H.-C. Chen, J.-X. Chen, Y.-C. Chen, I. A. Yu, and Y.-F. Chen, Phys. Rev. A **83**, 041804 (2011).
[23] R. B. Li, L. Deng, and E. W. Hagley, Phys. Rev. Lett. **110**, 113902 (2013).
[24] See e.g., S. E. Harris and L. V. Hau, Phys. Rev. Lett. **82**, 4611 (1999).
[25] J. Gea-Banacloche, Phys. Rev. A **81**, 043823 (2010).
[26] K. Hammerer, A. S. Sørensen, and E. S. Polzik, Rev. Mod. Phys. **82**, 1041 (2010).
[27] S. J. Buckle, S. M. Barnett, P. L. Knight, M. A. Lauder, and D. T. Pegg, Opt. Acta **33**, 1129 (1986).
[28] P. R. Hemmer, K. Z. Cheng, J. Kierstead, M. S. Shahriar, and M. K. Kim, Opt. Lett. **19**, 296 (1994).
[29] D. V. Kosachiov, B. G. Matisov, and Y. V. Rozhdestvensky, J. Phys. B **25**, 2473 (1992).
[30] The interface effective length (z) is essentially determined by the coupling beams waist through selective probing of the central portion of the transverse atoms distribution where the density is nearly uniform. The signal (control) beam [see Fig. 1(a)] is focused to the nearly uniform region of the atoms longitudinal density distribution with a confocal parameter larger than the ensemble length z to avoid unwanted diffraction effects. Short spatially uniform atomic "box-traps" [31,32] can also be used.
[31] T. Baluktsian, C. Urban, T. Bublat, H. Giessen, R. Löw, and T. Pfau, Opt. Lett. **35**, 1950 (2010).
[32] A. L. Gaunt, T. F. Schmidutz, I. Gotlibovych, R. P. Smith, and Z. Hadzibabic, Phys. Rev. Lett. **110**, 200406 (2013).
[33] See Supplemental Material at http://link.aps.org/supplemental/10.1103/PhysRevLett.115.113005 for details, which includes Refs. [34–38].
[34] A. J. Merriam, S. J. Sharpe, M. Shverdin, D. Manuszak, G. Y. Yin, and S. E. Harris, Phys. Rev. Lett. **84**, 5308 (2000).
[35] J.-H. Wu, M. Artoni, and G. C. La Rocca, Phys. Rev. A **82**, 013807 (2010).
[36] J.-H. Wu, M. Artoni, and G. C. La Rocca, Phys. Rev. A **81**, 033822 (2010).
[37] Y.-F. Hsiao, H.-S. Chen, P.-J. Tsai, and Y.-C. Chen, Phys. Rev. A **90**, 055401 (2014).
[38] D. A. Smith, S. Aigner, S. Hofferberth, M. Gring, M. Andersson, S. Wildermuth, P. Krüger, S. Schneider, T. Schumm, and J. Schmiedmayer, Opt. Express **19**, 8471 (2011).
[39] D. E. Chang, V. Vuletic, and M. D. Lukin, Nat. Photonics **8**, 685 (2014).
[40] A. M. C. Dawes, L. Illing, S. M. Clark, and D. J. Gauthier, Science **308**, 672 (2005).
[41] R. Loudon, *The Quantum Theory of Light* (Clarendon Press, Oxford, 2000).
[42] A. Zavatta, M. Artoni, D. Viscor, and G. La Rocca, Sci. Rep. **4**, 3941 (2014).
[43] M. Artoni and R. Loudon, Phys. Rev. A **57**, 622 (1998).
[44] The square $|Z(z,t)|^2$ represents the signal (m) mode space-time intensity distribution.
[45] I_{mm} is obtained from I_{mp} upon $\omega_p \to \omega_m$ and $\mathcal{E}^{\pm}(z,t) \to \mathcal{E}^{\pm}(z,t)(\mp 1 - 2\zeta)$.
[46] Such matching also requires coupling beams and wave packets of the same intensities and the resonance condition $\omega_m - \omega_{cm} = \omega_p - \omega_{cp}$, all clearly met here [Fig. 1(b)]. See, e.g., M. S. Shahriar and P. R. Hemmer Phys. Rev. Lett. **65**, 1865 (1990); W. Maichen, R. Gaggl, E. Korsunsky, and L. Windholz Europhys. Lett. **31**, 189 (1995).
[47] I. Bloch, J. Dalibard, and S. Nascimbene, Nat. Phys. **8**, 267 (2012).
[48] For definiteness we fix $\phi_m = 0$ (Fig. 2) so that $\Phi \to (\Delta\phi_c + \phi_p)/2$ and shift variations—for a set length z—can be equivalently achieved by changing either $\Delta\phi_c$ *or* ϕ_p.
[49] Such high densities can be achieved also with atom condensates or more sophisticated confinement geometries. See, e.g., S. Ghosh, A. R. Bhagwat, C. Kyle Renshaw, S. Goh, A. L. Gaeta, and B. J. Kirby, Phys. Rev. Lett. **97**, 023603 (2006).
[50] B. Lu, W. H. Burkett, and M. Xiao, Opt. Lett. **23**, 804 (1998).
[51] For $n_m = n_p$ the number of photons drops when computing $\arg[Z(z,t)]$ in Eq. (1).
[52] F. Lindner, G. G. Paulus, H. Walther, A. Baltuška, E. Goulielmakis, M. Lezius, and F. Krausz, Phys. Rev. Lett. **92**, 113001 (2004).
[53] Intensity lower bounds depend in principle only on the typical phase uncertainty associated with the signal (control) coherent state excitations we use here (See, e.g., Ref. [41] § 5.3).
[54] P. Coullet, L. Gil, and F. Rocca, Opt. Commun. **73**, 403 (1989).
[55] R. M. Camacho, P. B. Dixon, R. T. Glasser, A. N. Jordan, and J. C. Howell, Phys. Rev. Lett. **102**, 013902 (2009).
[56] T. Peyronel, O. Firstenberg, Q.-Y. Liang, S. Hofferberth, A. V. Gorshkov, T. Pohl, M. D. Lukin, and V. Vuletic, Nature (London) **488**, 57 (2012).
[57] V. Parigi, E. Bimbard, J. Stanojevic, A. J. Hilliard, F. Nogrette, R. Tualle-Brouri, A. Ourjoumtsev, and P. Grangier, Phys. Rev. Lett. **109**, 233602 (2012).
[58] C. Simon, Eur. Phys. J. D **58**, 1 (2010).
[59] V. Venkataraman, K. Saha, P. Londero, and A. L. Gaeta, Phys. Rev. Lett. **107**, 193902 (2011).
[60] M. Bajcsy, S. Hofferberth, T. Peyronel, V. Balic, Q. Liang, A. S. Zibrov, V. Vuletic, and M. D. Lukin, Phys. Rev. A **83**, 063830 (2011).
[61] M. W. Doherty, N. B. Manson, P. Delaney, F. Jelezko, J. Wrachtrup, and L. C. L. Hollenberg, Phys. Rep. **528**, 1 (2013).
[62] P. Ovartchaiyapong, K. W. Lee, B. A. Myers, and A. C. B. Jayich, Nat. Commun. **5**, 4429 (2014).
[63] E. R. MacQuarrie, T. A. Gosavi, N. R. Jungwirth, S. A. Bhave, and G. D. Fuchs, Phys. Rev. Lett. **111**, 227602 (2013).
[64] J.-M. Rost, Nat. Photonics **4**, 74 (2010).
[65] Q.-Y. He, Y. Xue, M. Artoni, G. C. La Rocca, J.-H. Xu, and J.-Y. Gao, Phys. Rev. B **73**, 195124 (2006).